IEEE Access
Multidisciplinary : Rapid Review : Open Access Journal

Received 20 December 2023, accepted 7 January 2024, date of publication 11 January 2024, date of current version 19 January 2024.

Digital Object Identifier 10.1109/ACCESS.2024.3352646

RESEARCH ARTICLE

A Novel Custom One-Dimensional Time-Series DenseNet for Water Pipeline Leak Detection and Localization Using Acousto-Optic Sensor

UMA RAJASEKARAN AND MOHANAPRASAD KOTHANDARAMAN
School of Electronics Engineering (SENSE), VIT University, Chennai, Tamil Nadu 600127, India

Corresponding author: Mohanaprasad Kothandaraman (kmohanaprasad@vit.ac.in)

This work was supported by Universiti Tunku Abdul Rahman, Sungai Long Campus, Kajang, Selangor, Malaysia, through the Trans-disciplinary Research Grant Scheme (TRGS) Project, under Grant TRGS/1/2016/UTAR/01/2/2.

ABSTRACT A crucial component within any structural health monitoring system is a pipeline leak detection mechanism, vital for preventing avoidable water loss. Contemporary literature employs machine learning and deep learning for detecting pipeline leaks and cross-correlation for leak localization. The major drawbacks in the existing methodologies are that machine learning and deep learning methods need two different architectures for leak detection and localization, and the cross-correlation needs two sensors with a denoising technique. The primary objective of this paper is to deploy a unified architecture capable of executing both the detection and localization of a leak without any denoising technique and with a single sensor. The proposed technique utilizes the data collected using an Acousto-optic sensor with two different pressures. This paper proposes a novel custom one-dimensional time-series DenseNet for leak detection and localization. The proposed method gives better accuracies compared with the existing one-dimensional DenseNet-121, three different one-dimensional convolutional neural networks (1DCNN), and cross-correlation for two different pressure datasets. The proposed method's processing time is thirteen times less than the existing one-dimensional DenseNet-121, with the observed average leak detection and localization accuracy of 99.08%. The results state that the proposed novel custom one-dimensional time-series DenseNet accurately detects and localizes the leak with less time.

INDEX TERMS Acousto-optic sensor, CNN, DenseNet, and pipeline leak detection and localization.

I. INTRODUCTION

Pipeline is the most considered mode of long-range water, oil, and gas transportation. The aging, wind, corrosion, and various external elements contribute to the degradation of this pipeline. As a result of this deterioration, leaks occur in the pipeline, leading to the loss of resources. An appropriate monitoring system is needed to identify the pipeline leak earlier to avoid wastage. Categorization of a few available pipeline leak detection and leak localization methods are external, visual/biological, and computational-based methods [1], [2]. This paper concentrates on pipeline leak detection and localization techniques using cross-correlation (CC), Machine Learning (ML) algorithms, and Deep Learning (DL) algorithms under computational-based leak detection and localization methods.

A few sensors applied in pipeline leak detection and leak localization are Acoustic Emission (AE), Acousto-optic sensor, spherical detector, flow meter, temperature sensor, and listening devices/microphones. The information obtained from the sensors in the real-time experimental arrangement contains noise. Few methods are available to denoise the signal collected from sensors. They are Empirical Mode Decomposition (EMD), Independent Component Analysis (ICA), Variational Mode Decomposition (VMD), Mel Frequency Cepstral Coefficients (MFCCs), Continuous Wavelet Transform (CWT), and Wavelet packet decomposition. After denoising, the cross-correlation localizes the leak by cross-referencing two sensor signals.

The associate editor coordinating the review of this manuscript and approving it for publication was Prakasam Periasamy.

ML algorithms like Support Vector Machine (SVM), Decision Tree (DT), Random Forest (RF), and K Nearest Neighbor (KNN) need feature extraction techniques. Feature extraction helps extract essential information from the raw or denoised data. DL algorithms like one-dimensional Convolutional Neural Networks (1DCNN), Deep Neural Networks (DNN), two-dimensional Convolutional Neural Networks (2DCNN), Artificial Neural Networks (ANN), and Long Short-Term Memory Auto Encoder (LSTM-AE) extract the features by itself from raw data or denoised data.

Xu et al. applied a leak detection approach using VMD-MFCC and SVM, incorporating a spherical detector for water pipelines [3]. The data collected from the spherical detector is noisy. The VMD denoises and MFCC help extract essential features for the SVM for leak detection. This VMD-MFCC and SVM gave an accuracy of 93%. Wang and Gao deployed a leak detection technique by integrating information from two acoustic and two pressure sensors, utilizing dual Pearson threshold ensemble EMD (DP-EEMD) and 1DCNN for water pipelines [4]. The acoustic and pressure signals undergo fusion and are subjected to DP-EEMD for noise reduction before employing the raw data for leak detection. Fusing data from two acoustic and two pressure sensors gave more accurate results.

Kim et al. implemented a leak detection method using a deep neural network for subsea gas pipelines with mass flow, pressure, and temperature [5]. The deep neural network model gave an accuracy of 80%. Ning et al. implemented an RF leak detection method for gas pipelines using listening devices [6]. The listening device captures the acoustic signals. The EEMD helped to denoise the captured acoustic signal, and a correlation coefficient helped to appropriate Intrinsic Mode Functions (IMFs). The features extracted from the denoised IMF are MFCC, time-domain and waveform features. The RF detects the leak with reasonable accuracy.

Spandonidis et al. studied 2DCNN and LSTM-AE using accelerometers to detect leaks in oil and gas pipelines [7]. The spectrograms of the accelerometers were the input for the 2DCNN, and the direct accelerometer signal was input to the LSTM-AE. The 2DCNN gave a better accuracy of 92%. Using accelerometer data, Yu et al. studied SVM, DT, KNN, and 2DCNN SqueezeNet for leak detection in water pipelines [8]. SVM, DT, and KNN detected the leak using features extracted from the accelerometer data. Meanwhile, for 2DCNN, the leak was identified by SqueezeNet using the spectrograms generated through the Short Time Fourier Transform. The 2DCNN SqueezeNet gave the highest accuracy of 95.15%.

Yang et al. implemented a leak detection model with 2DCNN using pressure sensor data [9]. To make the one-dimensional pressure data suitable for 2DCNN, Yang et al. utilized a CWT named Mortlet wavelet function. The Mortlet wavelet denoised the data and converted the one-dimensional data into two-dimensional data. The 2DCNN detected a leak with 97% average accuracy. Song and Li implemented a leak detection model using 2DCNN for the AE sensor data [10]. To make the one-dimensional acoustic sensor data compatible with 2DCNN, Song et al. utilized a CWT named DB8. Similar to the previously mentioned approach, the DB8 method denoised the data and transformed the one-dimensional data into a two-dimensional format. Utilizing the two-dimensional data, the 2DCNN successfully identified the leak with an accuracy of 93%.

Vanijjirattikhan et al. used microphones to compare SVM, 1DCNN, and DNN for water pipeline leak detection [11]. The one-dimensional time-domain data collected from the microphone is converted into a frequency domain using Fast Fourier Transform (FFT). The frequency domain data were then averaged and normalized before passing to the classifiers for leak detection. The analysis showed that the DNN outperformed the other two with 90% accuracy. Waleed et al. deployed a neural network to detect in-pipe leaks in oil and gas pipelines [12]. The in-pipe robot with three pressure sensors and an Arduino board helped collect data. Waleed et al. then performed an FFT operation on the collected one-dimensional pressure data before passing it to NN for classification. The NN classified the leak with reasonable accuracy.

From the above leak detection methods in ML and DL, it is evident that the ML and DL applications are for leak detection only. Still, the primary applied technique for the leak localization method is CC. Li et al. implemented a leak localization method in gas pipelines using two AE sensors [13]. This leak localization method included CC with an adaptive time-delay estimator. This method observed a relative error of 1% over an 80 m pipeline. The leak localization method implemented by Kothandaraman et al. is on Generalized CC (GCC) using two Acousto-optic sensors for water pipelines [14]. The noisy one-dimensional time-domain Acousto-optic sensor was denoised with adaptive ICA. GCC was performed on the denoised data to obtain the leak's location. This Adaptive ICA and GCC gave an accuracy of 93%.

Moreover, for enhanced precision in leak localization through the utilization of two acousto-optic sensors in water pipelines, Kothandaramam et al. integrated EMD in conjunction with Adaptive ICA to achieve superior noise removal [15]. The double-step noise-removed data was then performed with GCC to obtain leak localization. This method gave a leak localization accuracy of 96.47%. Furthermore, to improve the leak localization's accuracy, Kothandaramam et al. implemented a wavelet packet decomposition along with Adaptive ICA [16]. This method was again for water pipelines with two Acousto-optic sensors. This wavelet packet-based Adaptive ICA denoised well, and GCC localized leak with better accuracy.

The literature survey above indicates that ML and DL achieved superior accuracy among different sensors with more data for leak detection but not applied for localizing leaks. The widely applied tool for leak localization is cross-correlation. ML/DL and CC combined architectures are applied to perform detection and localization. Lang et al. implemented leak detection using Least Square Twin SVM (LSTSVM) and localization using CC for water pipelines [17]. The data utilized in this study was collected using pressure sensors with the Flowmaster software. The LMD helped to denoise the data for both detection and localization. Feature extraction for LSTSVM for leak detection from a single pressure sensor included time and frequency domain features. The leak was localized with CC from two pressure sensors after denoising. The observed detection and localization accuracies are 94.44% and 90.38%, respectively.

Zhou et al. explored a similar combined approach for water pipelines utilizing 2DCNN detection and CC for localization [18]. The data utilized in this study was also collected using pressure sensors with the Flowmaster software. The Improved Spline-Local Mean Decomposition (ISLMD) helped to denoise the data collected from the pressure sensors. Images of the denoised data from a single sensor are the input to 2DCNN for detection. Leak localized by CC with two denoised sensor data. Obtained leak detection and localization accuracies are 92.5% and 93.65%, respectively.

A few disadvantages observed from the literature survey are: 1) For detection and localization, two different architectures are needed, and 2) Localization using cross-correlation needs two sensors. These two different architectures and two sensors for localization increase the complexity. This paper proposes a novel custom one-dimensional time series DenseNet, a single architecture for leak detection and localization, with single Acousto-optic sensor data, and it does not need any noise removal process; this reduces the disadvantages of the existing systems. The paper organization is as follows: II) Related works, III) Experimental setup, IV) The proposed novel custom one-dimensional time-series DenseNet, V) Results and discussion, and VI) Conclusion.

II. RELATED WORKS

A. CONVOLUTIONAL NEURAL NETWORK (CNN)

CNN is a widely used tool for computer vision and natural language processing [19]. In recent years, applications of CNN have also extended pipeline leak detection with both one and two-dimensional. CNN is a feedforward architecture with many layers, and it learns with the help of filters, weights, and a bias. The optimizers aid in adjusting the weights during training, and the concurrent training of all layers minimizes the overall objective function [20]. The layers available in CNN are 1) the convolutional layer, 2) the max pool layer, 3) the fully connected layer, and the output layer. There are different activation functions available in CNN. Among them, 'ReLU' is a widely used activation function. Sample CNN architecture is in Fig. 1. The 'vanishing gradient' is the only drawback with 1DCNN. This problem increases as the number of layers in the CNN increases. It means specific data get lost while going for multiple convolutions.

CNN applied for pipeline leak detection and leak size classification. Kang et al. implemented an ensemble

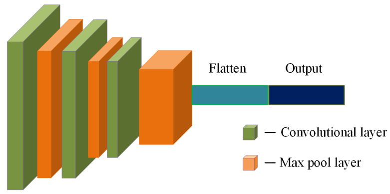

FIGURE 1. CNN architecture.

1DCNN-SVM for leak detection [21]. The ensemble includes MLP, and SVM detects the leak after extracting features from 1DCNN with a stochastic gradient descent optimizer. The 1DCNN ensemble architecture comprises an input layer, the initial convolutional layer with kernel and filter sizes of 32 and 64, succeeded by the first max-pooling layer with a pool size and a stride of 8 and 4, respectively. After this, the architecture splits into 1DCNN-SVM and Multi-Layer Perceptron (MLP). The Radial Basis Function is integrated into the 1DCNN-SVM, while the MLP features a dense layer with 256 neurons. Both 1DCNN-SVM and the MLP classify leaks, and the results are ensembled for optimized leak detection accuracy. Bohorquez et al. implemented a leak size detection and junction identification mechanism using 1DCNN [22]. The leak detection 1DCNN architecture comprises three convolutional layers with a leaky ReLU activation function, having layer sizes of 1200, 600, and 300, respectively. The filter size in each convolutional layer is 10. After the convolutional layer, the 1DCNN architecture contains three dense layers with 21, 9, and 2 neurons, respectively.

Ahmad et al. utilized 1DCNN to implement leak detection and identify leak sizes in fluid pipes using an acoustic emission sensor [23]. The architecture for leak detection and size identification using 1DCNN includes one input layer, five convolutional layers, four max pool layers, one dense layer, and one output layer. The architecture includes a first convolutional layer with a filter size 128 and a kernel size of 16, followed by the first max pool layer. The second convolutional layer has a filter size of 64 and a kernel size of 8, followed by the second max pool layer. In the third convolutional layer, the filter size is 32, and the kernel size is 4, followed by a max pool layer with a dropout ratio of 0.25. The fourth convolutional layer has a filter size of 16 and a kernel size of 4, followed by a max pool layer. Finally, the fifth convolutional layer has a filter size of 8 and a kernel size of 4, with a dropout ratio of 0.25, followed by a dense layer and an output layer. The number of neurons in the dense and output layers is 256 and 4, respectively. The 1DCNN gives good results in detecting leaks. Still, it has a vanishing gradient problem as there is an increase in the number of layers, the structure of the original data gets lost, and the architecture tends to overfit, resulting in poor prediction accuracy, F-score and R-squared error.

B. DENSENET-121

DenseNet is a type of CNN that utilizes dense connections between layers and addresses the 'vanishing gradient'

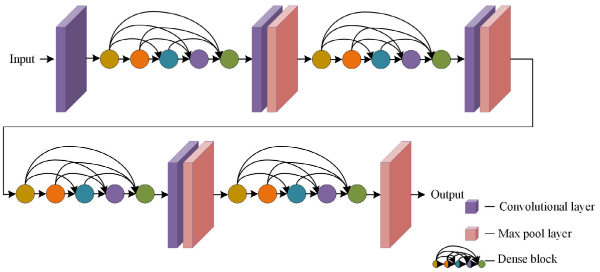

FIGURE 2. DenseNet-121 architecture.

problem. Apart from this, it has a few advantages: 1) feature propagation strengthening, 2) reusability of features, and 3) parameter reduction. A few drawbacks observed in DenseNet architecture are its massive number of trainable parameters that consume more memory and tremendous time to train, test and validate. One type of DenseNet that is available is DenseNet-121 [24]. The DenseNet-121 has 1) 1 - 7×7 convolutional layer, 2) 61 - 1×1 convolutional layer, 3) 58 - 3×3 convolutional layer, 4) 1 - max pool layer, 5) 4 - average pool layer, 6) 1 - fully connected layer, and 7) 1 - output layer. The architecture diagram of the DenseNet-121 is in Fig. 2

A few DenseNet applications are below; Zhang and Zhang applied DenseNet positively in their work to identify gas-liquid two-phase flow patterns with a resistance sensor array [25]. The data collected from the resistance sensor array was a one-dimensional time series. The Garmian Angular Field was pivotal in transforming the one-dimensional time-series data into a two-dimensional format. With the two-dimensional data, the implemented DenseNet architecture identifies four different flow patterns with 98.3% accuracy.

Kuo et al. implemented a DenseNet architecture to predict cutting tool wear with the NASA milling dataset [26]. The dataset consists of AE, vibration, and current sensor data. The DenseNet classified sixteen cutting tool wear cases with 0.06 mean absolute error and 0.09 mean squared error. Bakshi and Rajan implemented an Inception-based DenseNet for fall event detection with the SisFall dataset [27]. The SisFall dataset consists of fifteen fall cases and fifteen non-fall cases. The Short Time Fourier Transform was instrumental in converting the one-dimensional time series data into two-dimensional data. With two-dimensional data, the Inception-based DenseNet classified the fall event with a $97 \pm 4.7\%$ F-score.

III. THE PROPOSED NOVEL CUSTOM ONE-DIMENSIONAL TIME-SERIES DENSENET

The 1DCNN and the DenseNet are the most potent and predominant architectures. Even though both architectures have contributed to various types of classification with great accuracy, they have a few flaws. The 1DCNN gives good accuracy but has a vanishing gradient problem when layers increase and tend to overfit, leading to less prediction accuracy, F-score and R-squared error. The main advantage of the DenseNet is its efficiency in solving the vanishing gradient problem by helping the architecture maintain the data pattern, so the tendency to overfit is minimal. The only drawback with DenseNet is the tremendous number of trainable parameters and the time it takes to train, test, and validate. The 1DCNN is a lightweight architecture, whereas the DenseNet is heavy. The design of the proposed method brings both 1DCNN and DenseNet together by tailoring it to preserve the advantages of both architectures.

This paper proposes a novel custom one-dimensional time-series DenseNet combining 1DCNN and DenseNet. This architecture complements the advantages of both 1DCNN and DenseNet by eliminating the vanishing gradient problem with less trainable parameters. Further, the proposed architecture is a standalone model defined for leak detection and localization. The architecture diagram of the novel custom one-dimensional time-series DenseNet is in Fig. 3. The workflow of the proposed architecture is in Fig. 4.

Steps in proposed novel custom one-dimensional time-series DenseNet Architecture:

1) Fetch raw one-dimensional time-series data,
2) Learn features using 1DCNN blocks from the convolutional layer 1 to max pool layer 4,
3) Pass the learned features to the novel custom DenseNet block from convolutional layer 5 to convolutional layer 7,
4) Flatten the learned features to one-dimension and pass it to further dense layers,
5) Dense layers 1 and 2 help to reduce the number of features gradually and pass it to the output layer, and
6) The output layer helps detect and localize the leak based on the time the leak vibration signal takes to reach the sensor concerning the sensor's distance.

IV. EXPERIMENTAL SETUP

The experimental arrangement illustrated in Fig. 5 was employed to gather data for this research, comprising the following components,

1) A water storage unit of 1000 ltrs capacity,
2) A water pump,
3) A leak aperture of 5 mm,
4) Galvanized iron pipeline,
5) An Acousto-optic sensor,
6) A data acquisition unit and
7) A personal computer (PC).

The galvanized iron pipeline begins and concludes at the water storage unit, covering a distance of 40 meters. It possesses an internal diameter of 82 mm and an external diameter of 90 mm. The landscape vision of the experimental setup is in Fig. 6. Both Figs. 5 and 6 show how the experimental setup of a 40-meter pipeline is connected with a few small pipelines and elbow couplings and mounted from the floor. Pua et al.'s Acousto-optic sensor played a crucial role in gathering the data for this paper [28]. The schematic diagram of the Acousto-optic sensor can be found in Fig. 7, while the real-time image of the Acousto-optic sensor setup is in Fig 8.

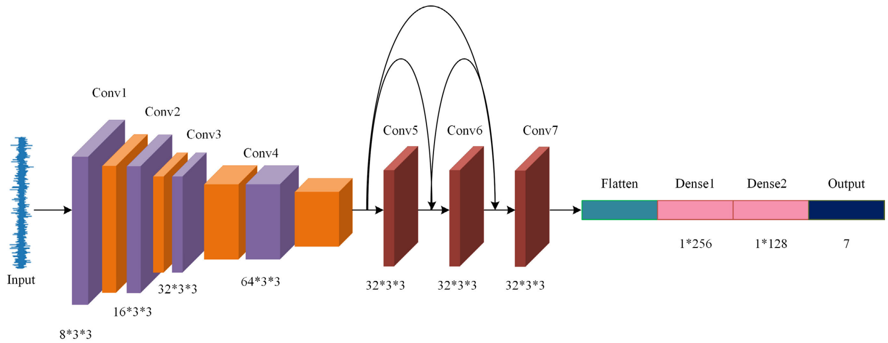

FIGURE 3. Architecture of proposed novel custom one-dimensional time-series DenseNet.

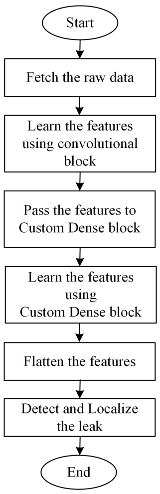

FIGURE 4. Workflow of the proposed novel custom one-dimensional time-series DenseNet.

FIGURE 5. Experimental setup.

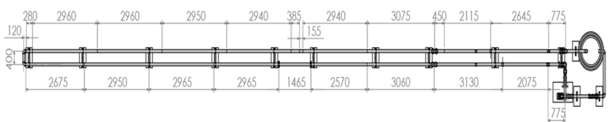

FIGURE 6. Landscape view of the experimental setup.

A. DATA COLLECTION

The experimental arrangement is in Fig. 5, and Fig. 6 illustrates the landscape view of the experimental setup. Fig. 7 showcases the configuration of the Acousto-optic sensor setup. At the same time, Fig. 8 features the placement of the sensing fiber of the Acousto-optic sensor on the leak aperture of the pipeline setup. It also contains the PicoScope,

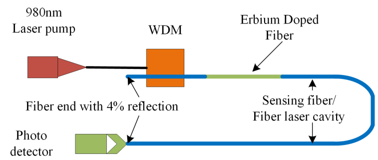

FIGURE 7. EDFL setup systematic diagram.

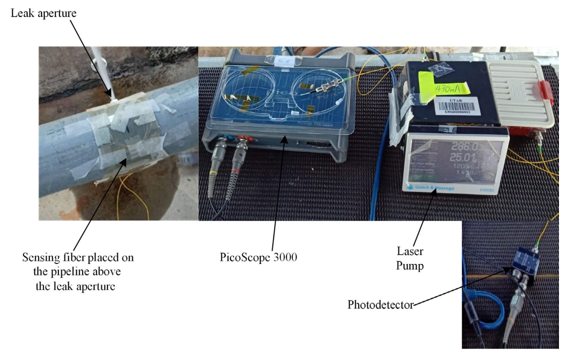

FIGURE 8. Acousto-optic sensor setup.

laser pump, and a photodetector. The sensing fiber is filled with laser particles with the help of the laser pump to make it suitable for observing the acoustic vibrations. The photodetector then observes the vibrated laser particles. The PicoScope and the PicoScope software on the PC connected at the photodetector's end helped collect data for this study. The data collected from the PicoScope is a one-dimensional time series. The leak aperture in the pipeline causes negative vibrations in the pipeline. The sensing fiber plays a crucial role in capturing these vibrations, while the PicoScope is instrumental in storing the observations for leak detection and localization analysis. The time taken for vibrations to reach the sensing fiber varies based on the distance at which the sensing fiber is on the pipeline. The design of the proposed architecture helps to understand the data pattern at different distances accordingly.

B. DATA DESCRIPTION

The dataset for this study contains seven sets with two different pressures. The pressures considered in this setup are 2bar and 3bar. The sensing fibers are positioned at

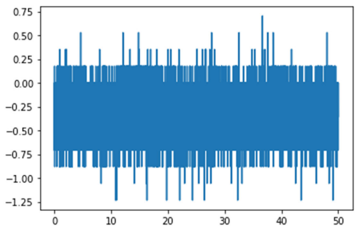

FIGURE 9. Sample of No-leak data.

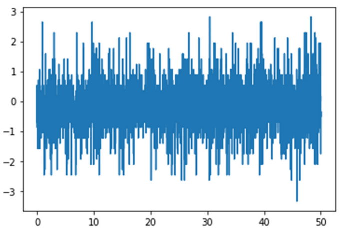

FIGURE 10. Sample of leak data at a 2-meter distance.

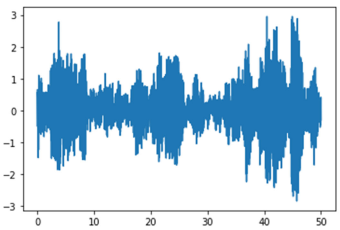

FIGURE 11. Sample of leak data at a 29-meter distance.

seven different lengths to gather data. The seven sets of data collected for this paper are as follows:

1) No-leak,
2) Leak at a.7-meter distance,
3) Leak at a 1-meter distance,
4) Leak at a 2-meter distance,
5) Leak at a 3-meter distance,
6) Leak at a 5-meter distance and
7) Leak at a 29-meter distance.

For the no-leak data, position the sensing fiber at a 1-meter distance from the leak aperture with the leak aperture closed. Additionally, collect data for the leak sets at their respective distances with an opened leak aperture. At a time, one sensor is placed at each distance, as listed above, with the leak aperture open to observe the vibrations in the pipeline. Each dataset category contains 1200 samples with 50 milliseconds duration. Therefore, there are 8400 samples in all categories. The ratio of dataset split of training, validation, and prediction is 80%, 16%, and 4%, respectively. For reference, sample images of data at 2bar pressure of no-leak, leak at a 2-meter distance, and leak at a 29-meter distance are shown in Figs. 9-11. Fig. 9. reflects the no-leak data containing only the vibrations of the pipeline when the leak aperture is closed. Figs. 10 and 11 reflect that the time taken for the leak vibration signal to reach the sensor differs based on the distance. From the Figs. 9-11, it is observed that there is a difference in amplitude between the leak and no-leak data.

V. ANALYSIS AND DISCUSSION

It is vital to visualize the benefits of DenseNet and 1DCNN architectures individually to understand the benefits of the proposed novel custom one-dimensional time-series DenseNet. So, this paper implements 1) one-dimensional DenseNet-121 [24], 2) Ensemble 1DCNN-SVM [21], 3) 1DCNN [22], 4) 1DCNN [23], 5) Proposed DenseNet architecture only, 6) Proposed 1DCNN architecture only, and 7) cross-correlation apart from the proposed novel custom one-dimensional time-series DenseNet. The one-dimensional DenseNet-121 [24], Ensemble 1DCNN-SVM [21], 1DCNN [22], and 1DCNN [23] are customized to have seven neurons in the final layer for the models to detect and localize leaks. The proposed DenseNet-only architecture comprises the following layers: 1) Convolutional layer 5, 2) Concatenation layer 1, 3) Convolutional layer 6, 4) Concatenation layer 2, 5) Convolutional layer 7, 6) Flatten layer, 7) Dense layer 1, 8) Dense layer 2, and 9) Output layer. On the other hand, the proposed 1DCNN-only architecture consists of the following layers: 1) Convolutional layer 1, 2) Max pool layer 1, 3) Convolutional layer 2, 4) Max pool layer 2, 5) Convolutional layer 3, 6) Max pool layer 3, 7) Convolutional layer 4, 8) Max pool layer 4, 9) Flatten layer, 10) Dense layer 1, 11) Dense layer 2, and 12) Output layer.

The metrics employed to assess all models, excluding cross-correlation, encompass the following: 1) time for training, validation, and prediction, 2) training accuracy (TA), 3) validation accuracy (VA), 4) prediction accuracy (PA), 5) precision, 6) recall, 7) specificity, 8) f-score, and 9) R squared, in conjunction with the total number of parameters. Total number of parameters in one-dimensional DenseNet-121 [24], Ensemble 1DCNN-SVM [21], 1DCNN [22], 1DCNN [23], Proposed DenseNet architecture only, Proposed 1DCNN architecture only, and the proposed novel custom one-dimensional time-series DenseNet are 5453255, 42084279, 2100529, 1346303, 83135367, 2041111, and 1784151, units respectively. As the cross-correlation needs two sensors for localization, the four best samples from the 1-meter cross-correlated with the four best samples from all the distance samples from both 2-bar and 3-bar pressures. Only average accuracy and R-squared are considered for cross-correlation, as other accuracy metrics are not applicable for cross-correlation.

Tables 1 and 2 contain the results for leak detection and localization under 2 and 3 bar pressures. Tables 4 and 5 give the confusion matrix of the proposed novel custom one-dimensional time-series DenseNet at 2 and 3 bar pressures, respectively. The results show that the proposed novel custom one-dimensional time-series DenseNet outperformed all the other mechanisms. While looking at the training, validation, and prediction accuracies, time, and number of parameters, the proposed 1DCNN performs better than 1D-DenseNet-121. On the contrary, while looking at the F-score and R-square, the 1D-DenseNet-121 performs better than the 1DCNN. These results clearly show that the proposed novel custom one-dimensional time-series DenseNet complements

TABLE 1. Results for leak detection and localization at 2 bar.

Sl no	Method	Time (minutes)	TA (%)	VA (%)	PA (%)	Precision	Recall/ sensitivity	Specificity	F-score	R-squared
1	1D-DenseNet-121 [24]	164.12	99.25	99.09	98.64	95.46	99.37	96.67	97.37	97.02
2	Ensemble 1DCNN-SVM [21]	4.39	26.25	25.81	22.72	22.72	99.99	0	37.03	16.73
3	1DCNN [22]	15.54	98.61	92.72	91.93	88.71	85.93	62.51	87.31	77.45
4	1DCNN [23]	18.71	98.89	97.73	96.93	93.91	96.35	87.51	95.11	90.61
5	Custom DenseNet-only	64.61	99.57	98.41	97.72	95.41	97.39	99.99	96.39	94.76
6	Custom 1DCNN-only	10.21	99.55	98.93	98.86	94.48	98.99	99.99	96.68	95.76
7	Traditional Cross-correlation	-	Average accuracy - 88.98%			-	-	-	-	97.17
8	**Proposed novel custom one-dimensional time-series DenseNet**	**4.76**	**99.29**	**99.09**	**98.95**	**95.97**	**99.47**	**96.87**	**97.69**	**98.01**

TABLE 2. Results for leak detection and localization at 3 bar.

Sl no	Method	Time (minutes)	TA (%)	VA (%)	PA (%)	Precision	Recall/ sensitivity	Specificity	F-score	R-squared
1	1D-DenseNet-121 [24]	162.02	98.29	97.73	96.93	92.75	99.99	68.75	96.24	95.17
2	Ensemble 1DCNN-SVM [21]	4.38	25.25	24.81	22.27	21.82	99.99	0	37.03	15.64
3	1DCNN [22]	15.46	98.39	91.02	90.12	87.06	91.14	18.75	89.05	68.53
4	1DCNN [23]	18.51	98.66	97.45	96.71	92.75	95.75	87.53	94.23	89.19
5	Custom DenseNet-only	64.71	98.55	96.82	95.91	93.51	97.39	71.87	95.41	90.53
6	Custom 1DCNN-only	10.28	99.34	98.57	97.38	93.91	96.35	93.75	95.11	92.32
7	Traditional Cross-correlation	-	Average accuracy - 87.91%			-	-	-	-	96.09
8	**Proposed novel custom one-dimensional time-series DenseNet**	**5.22**	**98.87**	**98.18**	**97.76**	**94.58**	**99.99**	**87.51**	**97.21**	**96.93**

TABLE 3. Confusion matrix of the proposed novel custom one-dimensional time-series DenseNet at 2 bar.

	No-leak	0.7 m	1 m	2 m	3 m	5 m	29 m	Accuracy of each class %
No-leak	192	0	0	0	0	0	0	100
0.7 m	0	188	4	0	0	0	0	97.91
1 m	0	0	191	1	0	0	0	99.47
2 m	0	0	9	183	0	0	0	95.31
3 m	0	0	0	0	192	0	0	100
5 m	0	0	0	0	0	192	0	100
29 m	0	0	0	0	0	0	192	100

TABLE 4. Confusion matrix of the proposed novel custom one-dimensional time-series DenseNet at 3 bar.

	No-leak	0.7 m	1 m	2 m	3 m	5 m	29 m	Accuracy of each class %
No-leak	191	0	1	0	0	0	0	99.47
0.7 m	0	181	11	0	0	0	0	94.27
1 m	0	0	192	0	0	0	0	100
2 m	0	0	18	174	0	0	0	90.62
3 m	0	0	0	0	192	0	0	100
5 m	0	0	0	0	0	192	0	100
29 m	0	0	0	0	0	0	192	100

the advantages of both DenseNet and 1DCNN in a very short time for both pressure datasets.

VI. CONCLUSION

The leak detection and localization mechanism for identifying pipeline leaks is crucial in every structural health monitoring system. The state-of-the-art approaches gave high leak detection accuracy using machine learning and deep learning. However, to localize the leak, the only available mechanism is cross-correlation. The cross-correlation also gives good accuracy in localizing leaks but with two sensors and an appropriate noise removal method. So, the existing method's complexity is very high. This paper proposed a novel custom one-dimensional time-series DenseNet, a standalone leak detection and localization architecture with reduced system complexity without any noise removal technique and cross-correlation. This paper also implemented the existing one-dimensional DenseNet-121, three variations of 1DCNN, and cross-correlation to check the credibility of the proposed method. The proposed novel custom one-dimensional time-series DenseNet outperforms all the other mechanisms. The number of parameters in the proposed novel custom one-dimensional time-series DenseNet is less compared with the existing one-dimensional DenseNet-121. To be precise, the number of parameters in the proposed method is approximately one-quarter of the existing one-dimensional DenseNet-121. The training time of the proposed method is also only one-thirteenth of the existing one-dimensional DenseNet-121. The proposed method and the one-dimensional DenseNet were trained, validated, and predicted with seven classes at two different pressures and gave an average accuracy of 99.08%, 98.63%, and 98.34%, respectively. Moreover, the results demonstrated that the proposed novel custom one-dimensional time-series DenseNet achieved more accurate leak detection and localization in a shorter time.

REFERENCES

[1] M. A. Adegboye, W.-K. Fung, and A. Karnik, "Recent advances in pipeline monitoring and oil leakage detection technologies: Principles and approaches," *Sensors*, vol. 19, no. 11, p. 2548, Jun. 2019, doi: 10.3390/s19112548.

[2] N. V. S. Korlapati, F. Khan, Q. Noor, S. Mirza, and S. Vaddiraju, "Review and analysis of pipeline leak detection methods," *J. Pipeline Sci. Eng.*, vol. 2, no. 4, Dec. 2022, Art. no. 100074, doi: 10.1016/j.jpse.2022.100074.

[3] T. Xu, Z. Zeng, X. Huang, J. Li, and H. Feng, "Pipeline leak detection based on variational mode decomposition and support vector machine using an interior spherical detector," *Process Saf. Environ. Protection*, vol. 153, pp. 167–177, Sep. 2021, doi: 10.1016/J.PSEP.2021.07.024.

[4] W. Wang and Y. Gao, "Pipeline leak detection method based on acoustic-pressure information fusion," *Measurement*, vol. 212, May 2023, Art. no. 112691, doi: 10.1016/J.MEASUREMENT.2023.112691.

[5] J. Kim, M. Chae, J. Han, S. Park, and Y. Lee, "The development of leak detection model in subsea gas pipeline using machine learning," *J. Natural Gas Sci. Eng.*, vol. 94, Oct. 2021, Art. no. 104134, doi: 10.1016/J.JNGSE.2021.104134.

[6] F. Ning, Z. Cheng, D. Meng, and J. Wei, "A framework combining acoustic features extraction method and random forest algorithm for gas pipeline leak detection and classification," *Appl. Acoust.*, vol. 182, Nov. 2021, Art. no. 108255, doi: 10.1016/J.APACOUST.2021.108255.

[7] C. Spandonidis, P. Theodoropoulos, F. Giannopoulos, N. Galiatsatos, and A. Petsa, "Evaluation of deep learning approaches for oil & gas pipeline leak detection using wireless sensor networks," *Eng. Appl. Artif. Intell.*, vol. 113, Aug. 2022, Art. no. 104890, doi: 10.1016/j.engappai.2022.104890.

[8] T. Yu, X. Chen, W. Yan, Z. Xu, and M. Ye, "Leak detection in water distribution systems by classifying vibration signals," *Mech. Syst. Signal Process.*, vol. 185, Feb. 2023, Art. no. 109810, doi: 10.1016/J.YMSSP.2022.109810.

[9] J. Yang, H. Mostaghimi, R. Hugo, and S. S. Park, "Pipeline leak and volume rate detections through artificial intelligence and vibration analysis," *Measurement*, vol. 187, Jan. 2022, Art. no. 110368, doi: 10.1016/J.MEASUREMENT.2021.110368.

[10] Y. Song and S. Li, "Gas leak detection in galvanised steel pipe with internal flow noise using convolutional neural network," *Process Saf. Environ. Protection*, vol. 146, pp. 736–744, Feb. 2021, doi: 10.1016/J.PSEP.2020.11.053.

[11] R. Vanijjirattikhan, S. Khomsay, N. Kitbutrawat, K. Khomsay, U. Supakchukul, S. Udomsuk, J. Suwatthikul, N. Oumtrakul, and K. Anusart, "AI-based acoustic leak detection in water distribution systems," *Results Eng.*, vol. 15, Sep. 2022, Art. no. 100557, doi: 10.1016/J.RINENG.2022.100557.

[12] D. Waleed, S. H. Mustafa, S. Mukhopadhyay, M. F. Abdel-Hafez, M. A. K. Jaradat, K. R. Dias, F. Arif, and J. I. Ahmed, "An in-pipe leak detection robot with a neural-network-based leak verification system," *IEEE Sensors J.*, vol. 19, no. 3, pp. 1153–1165, Feb. 2019, doi: 10.1109/JSEN.2018.2879248.

[13] S. Li, Y. Wen, P. Li, J. Yang, and L. Yang, "Leak detection and location for gas pipelines using acoustic emission sensors," in *Proc. IEEE Int. Ultrason. Symp. (IUS)*, Oct. 2012, pp. 957–960, doi: 10.1109/ULTSYM.2012.0239.

[14] M. Kothandaraman, Z. Law, E. M. A. Gnanamuthu, and C. H. Pua, "An adaptive ICA-based cross-correlation techniques for water pipeline leakage localization utilizing acousto-optic sensors," *IEEE Sensors J.*, vol. 20, no. 17, pp. 10021–10031, Sep. 2020, doi: 10.1109/JSEN.2020.2991639.

[15] M. Kothandaraman, Z. Law, M. A. G. Ezra, and C. H. Pua, "Adaptive independent component AnalysisBased cross-correlation techniques along with empirical mode decomposition for water pipeline leakage localization utilizing acousto-optic sensors," *J. Pipeline Syst. Eng. Pract.*, vol. 11, no. 3, Aug. 2020, Art. no. 04020027, doi: 10.1061/(asce)ps.1949-1204.0000471.

[16] M. Kothandaraman, Z. Law, M. A. G. Ezra, C. H. Pua, and U. Rajasekaran, "Water pipeline leak measurement using wavelet packet-based adaptive ICA," *Water Resour. Manage.*, vol. 36, no. 6, pp. 1973–1989, Mar. 2022, doi: 10.1007/S11269-022-03119-Y.

[17] X. Lang, P. Li, Z. Hu, H. Ren, and Y. Li, "Leak detection and location of pipelines based on LMD and least squares twin support vector machine," *IEEE Access*, vol. 5, pp. 8659–8668, 2017, doi: 10.1109/ACCESS.2017.2703122.

[18] M. Zhou, Z. Pan, Y. Liu, Q. Zhang, Y. Cai, and H. Pan, "Leak detection and location based on ISLMD and CNN in a pipeline," *IEEE Access*, vol. 7, pp. 30457–30464, 2019, doi: 10.1109/ACCESS.2019.2902711.

[19] A. Ghosh, A. Sufian, F. Sultana, A. Chakrabarti, and D. De, "Fundamental concepts of convolutional neural network," in *Recent Trends and Advances in Artificial Intelligence and Internet of Things*. Cham, Switzerland: Springer, 2020, pp. 519–567, doi: 10.1007/978-3-030-32644-9_36.

[20] F. J. Huang and Y. LeCun, "Large-scale learning with SVM and convolutional for generic object categorization," in *Proc. IEEE Comput. Soc. Conf. Comput. Vis. Pattern Recognit. (CVPR)*, vol. 1, Jun. 2006, pp. 284–291, doi: 10.1109/CVPR.2006.164.

[21] J. Kang, Y.-J. Park, J. Lee, S.-H. Wang, and D.-S. Eom, "Novel leakage detection by ensemble CNN-SVM and graph-based localization in water distribution systems," *IEEE Trans. Ind. Electron.*, vol. 65, no. 5, pp. 4279–4289, May 2018, doi: 10.1109/TIE.2017.2764861.

[22] J. Bohorquez, B. Alexander, A. R. Simpson, and M. F. Lambert, "Leak detection and topology identification in pipelines using fluid transients and artificial neural networks," *J. Water Resour. Plan Manag.*, vol. 146, no. 6, Apr. 2020, Art. no. 04020040, doi: 10.1061/(ASCE)WR.1943-5452.0001187.

[23] Z. Ahmad, T.-K. Nguyen, and J.-M. Kim, "Leak detection and size identification in fluid pipelines using a novel vulnerability index and 1-D convolutional neural network," *Eng. Appl. Comput. Fluid Mech.*, vol. 17, no. 1, Dec. 2023, Art. no. 2165159, doi: 10.1080/19942060.2023.2165159.

[24] G. Huang, Z. Liu, L. Van Der Maaten, and K. Q. Weinberger, "Densely connected convolutional networks," in *Proc. IEEE Conf. Comput. Vis. Pattern Recognit. (CVPR)*, Jul. 2017, pp. 2261–2269, doi: 10.1109/CVPR.2017.243.

[25] L. Zhang and S. Zhang, "Gas/liquid two-phase flow pattern identification method using Gramian angular field and densely connected network," *IEEE Sensors J.*, vol. 23, no. 4, pp. 4022–4032, Feb. 2023, doi: 10.1109/JSEN.2023.3235954.

[26] P.-H. Kuo, C.-Y. Lin, P.-C. Luan, and H.-T. Yau, "Dense-block structured convolutional neural network-based analytical prediction system of cutting tool wear," *IEEE Sensors J.*, vol. 22, no. 21, pp. 20257–20267, Nov. 2022, doi: 10.1109/JSEN.2022.3206308.

[27] S. Bakshi and S. Rajan, "Fall event detection system using inception-densenet inspired sparse Siamese network," *IEEE Sensors Lett.*, vol. 5, no. 8, pp. 1–4, Aug. 2021, doi: 10.1109/LSENS.2021.3089619.

[28] C. H. Pua, H. Ahmad, S. W. Harun, and R. M. De La Rue, "Study of dual-wavelength mode competition in an erbium-doped fiber laser (EDFL) produced by acoustic waves," *IEEE J. Quantum Electron.*, vol. 48, no. 12, pp. 1499–1504, Dec. 2012, doi: 10.1109/JQE.2012.2219505.

UMA RAJASEKARAN was born in 1986. She received the Bachelor of Engineering degree from the Department of Electronics and Communication Engineering, Tamilnadu College of Engineering, Coimbatore, Tamil Nadu, in 2007, the Master of Engineering degree in industrial engineering from the PSG College of Technology, Coimbatore, in 2012, and the Master of Engineering degree in communication systems from Vels University, Chennai, Tamil Nadu, in 2018. She is currently pursuing the Ph.D. degree with the School of Electronics Engineering, VIT University, Chennai. Her research interests include signal processing, machine learning, and deep learning.

MOHANAPRASAD KOTHANDARAMAN was born in 1981. He received the Bachelor of Engineering degree from the University of Madras, Chennai, the Master of Engineering degree from Anna University, Chennai, in 2006, and the Ph.D. degree in speech signal processing from VIT University, Vellore, India, in 2016. He held a Postdoctoral Research Fellowship with UTAR Malaysia. Currently, he is an Associate Professor (Senior) with the School of Electronics Engineering, VIT University, Chennai. He has more than 30 international journals and international conference publications. His research interests include signal processing, acoustic speech processing, deep learning, and natural language processing.